

THE COMPLEMENTARY RELATIONSHIP IN REGIONAL EVAPOTRANSPIRATION:  
THE CRAE MODEL AND THE ADVECTION-ARIDITY APPROACH

Michael T. Hobbins<sup>1</sup>, Jorge A. Ramírez<sup>2</sup>, and Thomas C. Brown<sup>3</sup>

**ABSTRACT**

Two implementations of *Bouchet's* [1963] hypothesis—*Morton's* Complementary Relationship Areal Evapotranspiration (CRAE) model and *Brutsaert and Stricker's* Advection-Aridity (AA) model—for regional evapotranspiration are evaluated against independent estimates derived from long-term (1962-1988), large-scale water balances for minimally impacted river basins in the conterminous US.

The CRAE model [*Morton*, 1983] is shown to be a powerful tool in estimating regional evapotranspiration at a monthly time-scale, yielding unbiased estimates with a mean annual water balance closure error of –1.32%. The AA model in the formulation proposed by *Brutsaert and Stricker* [1979] using the Penman wind function [*Penman*, 1948] yields evapotranspiration estimates that are biased towards underestimation: the mean error is 8.95%. Both models over-estimate evapotranspiration in arid basins. In general, increasing humidity leads to decreasing absolute closure errors for both models, while increasing aridity leads to increasingly negative CRAE closure errors and independently high positive AA closure errors.

The significant differences in the models' performances are due primarily to the use of the concept of equilibrium temperature in the CRAE model and its effects on the surface radiation budget, and to the choice of wind function in the AA model, which is highly dependent on the advective portion of its formulation. An attempt to improve the AA model by seasonally recalibrating the wind function led to significant differences from the original Penman wind function for the growing season, but did not yield improvements in the performance of the model as regards long-term, large-scale water balances.

**INTRODUCTION**

While the physics of energy and mass transfer at the land surface-atmosphere interface can be successfully modeled at a small scale [*Katul and Parlange*, 1992; *Parlange and Katul*, 1992a; *Parlange and Katul*, 1992b], our understanding of these processes at the larger—or regional—scale necessary for use by hydrologists, water managers, and climate modelers is limited. Consequently, our ability to estimate regional evapotranspiration has been

---

<sup>1</sup> M.S. Student, Civil Engineering Dept., Colorado State University, Fort Collins, CO 80523,

<sup>2</sup> Associate Professor, Civil Engineering Dept., Colorado State University, Fort Collins, CO 80523

<sup>3</sup> Faculty Affiliate, Colorado State University. Economist, Rocky Mountain Research Station, U. S. Forest Service, Fort Collins, CO 80526

constrained by models that treat potential evapotranspiration ( $ET_p$ ) as an independent climatic forcing process and derive actual evapotranspiration ( $ET_a$ ) estimates through non-physical, empirical relationships thereof.

The theory of the complementary relationship in regional evapotranspiration, first proposed by *Bouchet* [1963], considers  $ET_p$  a function of feedback processes between limitations of water availability at the land surface and the evaporative power of the overlying atmosphere, and estimates  $ET_a$  using data that describe the conditions of the over-passing air. Two implementations of this hypothesis are examined in large-scale, long-term water balances for a variety of climatic conditions in the conterminous United States.

### COMPLEMENTARY RELATIONSHIP MODELS

*Bouchet's* [1963] hypothesis states that, for uniform surfaces of a regional scale (scale lengths of the order of 1-10km) and in the absence of oasis effects and other sharp environmental discontinuities, when the actual evapotranspiration rate ( $ET_a$ ) is limited by both the energy input and the moisture available at the surface, then the potential evapotranspiration ( $ET_p$ ) is increased by the same amount.

This hypothesis assumes a well mixed atmospheric sub-layer and that only temperature, humidity and turbulence in the equilibrium sub-layer are affected: the net radiation at surface is not affected. The hypothesis leads to the three measures of evaporation following and shown in Figure 1:

- i.  $ET_w$ , Wet Environment Evaporation: rate under conditions where the only limitation is the availability of energy;
- ii.  $ET_a$ , Actual Evapotranspiration: occurs under moisture-limited conditions;
- iii.  $ET_p$ , Potential Evapotranspiration: theoretical rate under moisture-limited conditions if the resulting excess in surface energy budget could be used to evaporate further moisture.

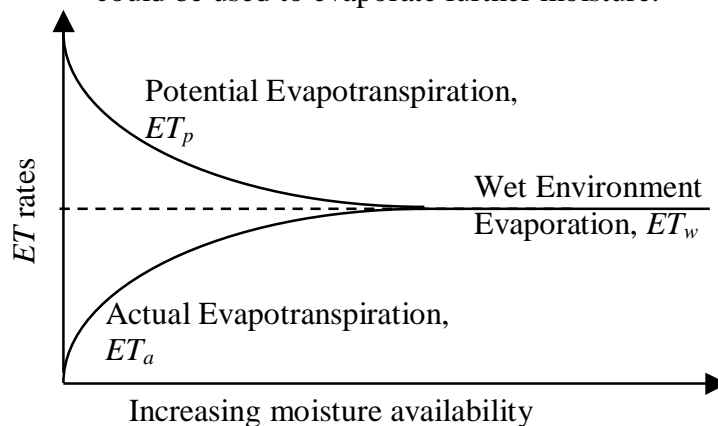


**Figure 1.** Conceptualization of complementary relationship under conditions of constant energy supply.

Estimates of regional evapotranspiration under the complementary relationship hypothesis are then described by equation (1).

$$ET_a = 2ET_w - ET_p \quad (1)$$

The main advantage of these models is that they rely solely on routine climatological observations. Local temperature and humidity gradients in the atmospheric boundary layer respond to—and obviate the necessity for information regarding—the conditions of moisture availability at the surface. The models bypass the complex and poorly understood soil-plant processes, and thus do not require data on soil moisture, stomatal resistance properties of the vegetation, or any other aridity measures. Neither do they require local calibration of parameters, beyond those built in to the models.

The two most significant differences between the two models are observed in their treatments of temperature and advection. The CRAE model uses “equilibrium temperature”  $T_p$  (see below) to approximate the surface temperature and adjusts the surface energy budget for long-wave back-radiation and sensible heat at  $T_p$ . The AA model calculates the energy budget at air temperature  $T_a$ . With regard to advection, the CRAE model uses a constant vapor transfer coefficient  $f_T$ , which is simply a function of atmospheric pressure and is independent of actual wind speed, whereas the AA model uses a wind function  $f(U_2)$ , which is an empirical function of observed wind speed.

Potential evapotranspiration  $ET_p$ : Both models use information from the energy budget and the water vapor transfer equations. The AA model uses the *Penman* [1948] “combination equation” (2), a convex linear combination of two forces driving evapotranspiration: that due to net radiation  $R_n$  at the evaporating surface; and that due to the drying power of advected air  $E_a$ . The CRAE model decomposes the Penman equation into the two components, and postulates a theoretical “equilibrium temperature”  $T_p$ , the temperature at which the mass transfer equation (3a) yields the same result as the  $T_p$ -corrected energy budget equation (3b).

$$\lambda ET_p^{AA} = \frac{\Delta}{\Delta + \gamma} R_n + \frac{\gamma}{\Delta + \gamma} E_a \quad (2)$$

$$\lambda ET_p^{CRAE} = f_T (e_p^* - e_a) \quad (3a)$$

$$\lambda ET_p^{CRAE} = R_n - [\lambda f_T + 4\epsilon\sigma T_p^3] (T_p - T_a) = R_n - \lambda f_T (T_p - T_a) \quad (3b)$$

Wet environment evaporation,  $ET_w$ : Both models use formulations derived from the *Priestley and Taylor* [1972] equilibrium evaporation: the AA model uses the unadulterated Priestley-Taylor expression (4), whereas the CRAE model increases the available energy for evaporation by a globally calibrated, empirical advection term  $b_1$ , replaces the Priestley-Taylor coefficient  $\alpha$  by  $b_2$ , and adjusts the surface energy budget for long-wave back-radiation at  $T_p$  (5).

$$\lambda ET_w^{AA} = \alpha \frac{\Delta}{\Delta + \gamma} R_n \quad (4)$$

$$\lambda ET_w^{CRAE} = b_1 + b_2 \frac{\Delta_p}{\Delta_p + \gamma} \left[ R_n - 4\epsilon\sigma T_p^3 (T_p - T_a) \right] \quad (5)$$

### WATER BALANCES USING INITIAL MODELS

The objective of the study is to compare  $ET_a$  estimates from the CRAE and AA models with independent evapotranspiration estimates ( $ET_a^*$ ) provided by long-term, large-scale water budgets for undisturbed basins in the conterminous United States. The errors invoked are examined as they relate to climatological and physical basin characteristics. Finally, improvements are suggested to the AA model as regards advection.

Long-term, large-scale water balances for undisturbed basins reduce to:

$$ET_a^* = P - R \quad (6)$$

where  $P$  is precipitation and  $R$  is surface runoff.

The water balance evapotranspiration estimates  $ET_a^*$  are calculated for 139 undisturbed basins across the conterminous United States on a monthly basis for water years 1962-1988. The basins are selected from the data set “Hydro-climatic Data Network (HCDN)” [Slack and Landwehr, 1992]. These basins contain a total of 362 HUC’s, and cover 17.5% of the total area of the conterminous United States. Corresponding precipitation and streamflow data are obtained from the spatially distributed data sets “Parameter-elevation Regressions on Independent Slopes Model (PRISM)” [Daly *et al.*, 1994], and the U.S. Geological Survey (USGS) “Hydro-Climatic Data Network (HCDN)” [Slack and Landwehr, 1992], respectively.

It is assumed that inter- and intra-basin diversions and groundwater pumping are insignificant. In addition to having a relatively low level of intra-basin diversion, Ramírez and Claessens [1994] concluded, based on two USGS inter-basin transfer inventories, that the gaged basins used in this study are only minimally affected by inter-basin diversions.

The model evapotranspiration estimates ( $ET_a^{CRAE}$  and  $ET_a^{AA}$ ) require data on average temperature, solar radiation, wind speed, humidity, albedo, and elevation. Temperature data are drawn from “NCDC Summary of the Day” [EarthInfo, 1998a], and average temperature is estimated as the mean of the average monthly maximum and average monthly minimum temperatures. Solar radiation and wind speed data are drawn from “Solar and Meteorological Surface Observation Network (SAMSON)” [NREL, 1993]. Humidity data, in the form of dew-point temperatures, are drawn from “NCDC Surface Airways” [EarthInfo, 1998b]. Average monthly albedo surfaces are AVHRR-derived estimates from the Gutman [1988] data set.

For the 27 water years 1962-1988, monthly surfaces are constructed for wind speed, solar radiation, dewpoint temperature and average temperature. These surfaces are used as inputs to the two models, and monthly surfaces of the three components of the complementary relationship are created as output. The  $ET_a^{MODEL}$  estimates are temporally integrated across the record length, spatially integrated across the extent of each of the 139 basins under study, and the resulting accumulated volumes of evapotranspired water are compared with the water balance estimate ( $ET_a^*$ ).

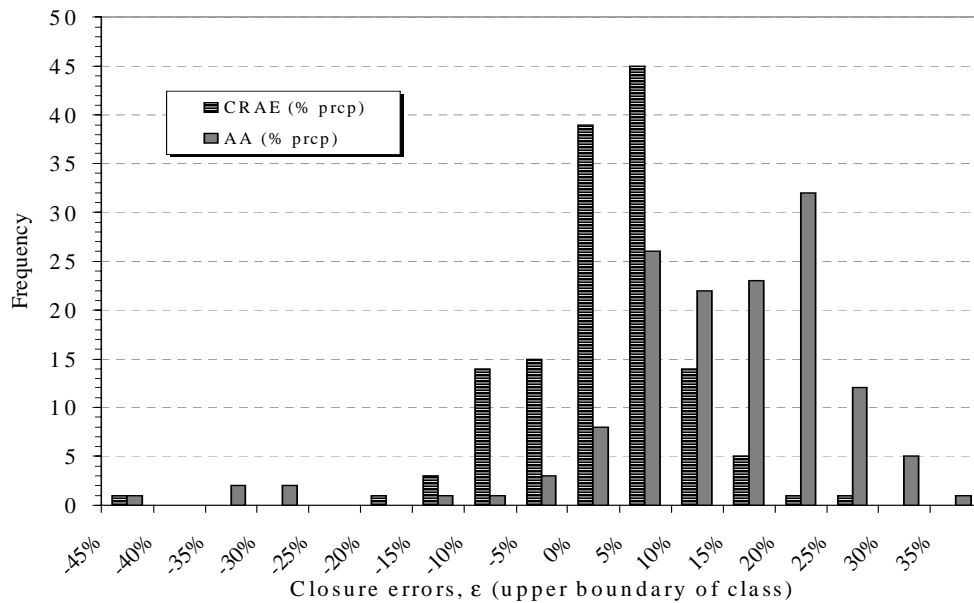
The average annual water balance closure error  $\epsilon$  is calculated for each basin, as a percentage of average annual precipitation, from equation (7):

$$\epsilon = \frac{\sum_{i=1}^{27} \sum_{j=12}^{12} (ET_{a(i,j)}^* - ET_{a(i,j)}^{MODEL})}{\sum_{i=1}^{27} \sum_{j=12}^{12} P_{(i,j)}} * 100\% \quad (7)$$

where  $ET_a^{MODEL}$  is the model estimate of  $ET_a$  (i.e.,  $ET_a^{AA}$  or  $ET_a^{CRAE}$ ), and  $i$  and  $j$  are the water year and month, respectively. Thus, a positive closure error indicates that the aggregated  $ET_a^*$  exceeds  $ET_a^{MODEL}$ , and the model is underestimating  $ET_a$ . A negative closure error indicates the opposite.

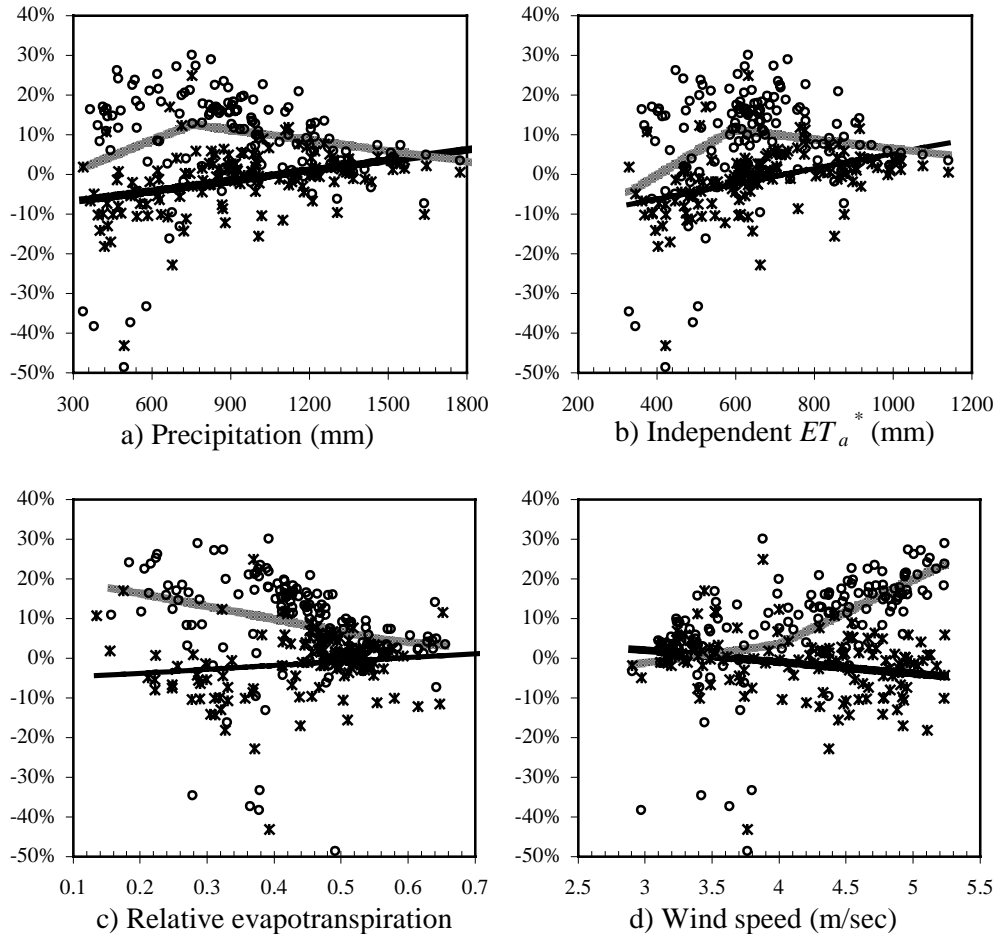
## RESULTS FOR INITIAL MODELS

Figure 2 shows the empirical distribution of water balance closure errors for the CRAE and AA models. Disregarding the outliers at  $-45\%$ , the range is approximately  $\pm 35\%$ . For the CRAE model, the closure errors are normally distributed, with mean  $-1.32\%$  and standard deviation  $7.76\%$ . The distribution of the closure errors for the AA model is bi-modal—with modes at  $5\%$  and  $25\%$ —and skewed to the left. The mean is  $8.95\%$ , and the variability is greater than the CRAE model: the standard deviation is  $12.71\%$ .



**Figure 2.** Distribution of water balance closure errors,  $\epsilon^{CRAE}$  and  $\epsilon^{AA}$ .

Figures 3a through 3c depict the effects of basin climatology upon the performance of the models, as measured by the water balance closure errors  $\epsilon^{CRAE}$  and  $\epsilon^{AA}$ . Each of the dependent variables is a measure of aridity and/or humidity of the basin, with aridity increasing toward the left in each graph. In each of these cases, the CRAE model exhibits the same behavior:  $\epsilon^{CRAE}$  increases slightly and converges with humidity. Of greater interest is the behavior of the AA model.



**Figure 3.** Relationships of  $\epsilon^{CRAE}$  (x) and  $\epsilon^{AA}$  (o) to basin climatological characteristics: (a) Precipitation; (b) Independent evapotranspiration estimate  $ET_a^*$ ; (c) Relative evapotranspiration; (d) Wind speed. Independent variables are mean annual basin-wide quantities. Regression lines (black for  $\epsilon^{CRAE}$ , grey for  $\epsilon^{AA}$ ) are for trend observations only.

For mean annual precipitation (Figure 3a) totals less than 750mm/year,  $\epsilon^{AA}$  is positive but independent of precipitation, indicating that  $ET_a^{AA}$  underestimates with aridity. For totals greater than 750mm/year,  $\epsilon^{AA}$  converges toward zero, implying that the  $ET_a^{AA}$  estimates improve with humidity.

Figure 3b indicates the relationship between  $\epsilon^{MODEL}$  and the independent estimates  $ET_a^*$ , provided by equation (6). For  $ET_a^*$  totals less than 585mm/year,  $\epsilon^{AA}$  is positive and independent of  $ET_a^*$ , and the scatter increases with aridity, implying that  $ET_a^{AA}$  underestimates with increasing aridity. For  $ET_a^*$  totals greater than 585mm/year,  $\epsilon^{AA}$  converges toward zero, implying that the  $ET_a^{AA}$  estimate improves with humidity.

Relative  $ET$ —the ratio of  $ET_a$  to  $ET_p$ —is a direct measure of saturation of the basin land surface. Increasing this ratio is equivalent to moving to the right in Figure 1:  $ET_a$  and  $ET_p$  converge towards  $ET_w$ . Figure 3c indicates that  $\epsilon^{AA}$  decreases and converges to zero with increasing humidity.

The relationship between  $\epsilon^{MODEL}$  and mean annual basin wind speed (Figure 3d) indicates that  $\epsilon^{CRAE}$  are weakly negatively correlated with wind speed, tending to be clustered around zero. This supports *Morton's* [1983] treatment of advection in the CRAE model.  $\epsilon^{AA}$  are strongly positively correlated with—and hence the AA model is very sensitive to—wind speed, especially for wind speeds above 4 m/sec. In fact,  $U_2$  exhibits the strongest relationship with  $\epsilon^{AA}$  of any climatic variable. The first step in improving the AA model must necessarily be to re-parameterize the wind function  $f(U_2)$ .

#### ADVECTION AND THE COMPLEMENTARY RELATIONSHIP MODELS

In the combination approach (2), the mass transfer of vapor is represented by an aerodynamic vapor transfer term  $E_a$ : a multiple of the vapor pressure deficit ( $e_a^* - e_a$ ) and a function of the speed of the advected air  $f(U_2)$ , of the form (8):

$$E_a = f(U_2)(e_a^* - e_a) \quad (8)$$

In general, the wind function  $f(U_r)$  is either theoretically or empirically derived. *Brutsaert and Stricker* [1979] suggested the following theoretical expression (9) for the wind function under neutral conditions:

$$f(U_r) = \frac{a_v k^2 \rho U_r}{\ln[(z_r - d)/z_o] \ln[(z_r - d)/z_{ov}]} \quad (9)$$

where wind speed  $U_r$  is observed at height  $r$ (m) above the ground,  $a_v$  is the ratio of the eddy diffusivity to the eddy viscosity,  $k$  is the von Karman constant,  $\rho$  is the air density,  $d$  is the displacement height, and  $z_o$  and  $z_{ov}$  are the roughness lengths for momentum and water vapor, respectively.

However, in the context of modeling monthly  $ET_a$  with the complementary relationship, the effects of atmospheric instability and the onerous data requirements rule out such theoretical formulations. *Penman* [1948] originally suggested the following empirical formulation (10) for  $f(U_2)$ :

$$f(U_2) = 0.35(1 + 0.54U_2)(e_a^* - e_a) \quad (10)$$

for wind speeds at 2m elevation in m/sec, vapor pressures in mmHg, yielding  $E_a$  in mm/day. In the agricultural arena, much work has been done to

calibrate or re-formulate the proposed wind function for use in the combination or Penman equation (e.g., *Allen* [1986], *Van Bavel* [1966], *Wright* [1982]). These agriculturally oriented formulations operate on a limited spatial and temporal scale, do not hypothesize feedbacks of a regional nature, and require local parameterizations of resistance and canopy roughness. Thus, they are not applicable in the setting of predicting regional evapotranspiration.

The CRAE model uses a vapor transfer coefficient  $f_T$  (11) dependent solely on atmospheric pressure, because [*Morton*, 1983]:  $f_T$  increases with both surface roughness and atmospheric instability, but wind speed is negatively correlated with both of these; and observations of  $U_2$  are unreliable, due to instrument and station variability.

$$f(U_z) \approx f_T = \left( \frac{p_0}{p} \right)^{0.5} f_z \zeta^{-1} \quad (11)$$

Here,  $f_z$  is a globally calibrated parameter,  $\zeta$  is a dimensionless stability factor, and  $p$  and  $p_0$  are station and sea-level atmospheric pressures, respectively.

In light of the strong relationship between mean annual wind speed and  $\epsilon^{AA}$  (see Figure 3d), an independent method for re-parameterizing the wind function  $f(U_2)$  is presented.

At a point in a homogeneous region of scale lengths on the order of 1-10km, the complementary relationship indicates that a free-water surface will evaporate at the potential rate  $ET_p$ . Thus, if the aerological conditions are known (i.e, temperature, humidity, and solar radiation), then pan evaporation ( $ET_{pan}$ ) data can be used to back-calculate the value of the drying power of the air  $E_a$ , and hence, the value of the wind function  $f(U_2)$ , using equation (12).

$$f(U_2) = \left( ET_{pan} - \frac{\Delta}{\Delta + \gamma} R_n \right) \frac{\Delta + \gamma}{\gamma(e_a^* - e_a)} \quad (12)$$

Here,  $ET_p^{AA}$  in (2) is replaced by  $ET_{pan}$ , and the resulting expression can be used on a seasonal (i.e., monthly) basis to back-calculate the required value of the wind function  $f(U_2)$ , which may then be combined with the observed wind speeds at the station to generate an empirical  $U_2$ - $f(U_2)$  relationship.

Monthly pan evaporation ( $ET_{pan}$ ) data are drawn from 14 stations across the conterminous United States in the data set ‘‘NCDC Summary of the Day’’ [*EarthInfo*, 1998a]. These stations are then matched to the closest (i.e., within 1 minute Lat/Long) reporting SAMSON stations [*NREL*, 1993], from which the other climatological input data (average temperature, solar radiation, and humidity) are drawn. The resulting  $f(U_2)$  values are then compared, on a monthly basis, to the wind speeds observed at the SAMSON stations. For each month, a least-squares fit is derived to express this



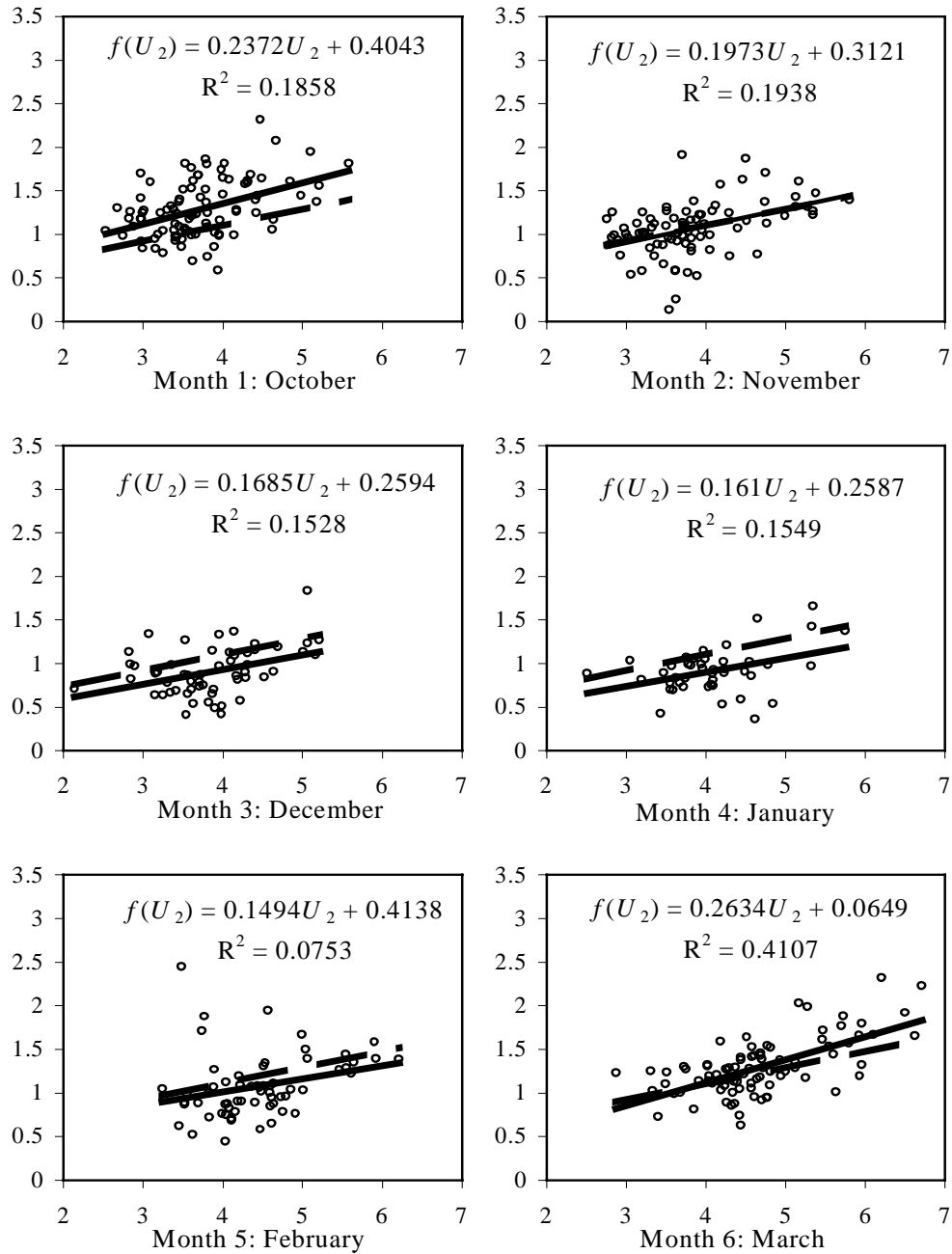


**Figure 4.** Monthly  $f(U_2)$ - $U_2$  relationships: months 1-6. Solid line is least-squares fit, with equation and  $R^2$  value indicated. Penman wind function from equation (10) shown by dashed line.

relationship, and these are shown in Figure 4. Also shown in Figure 4 is the wind speed-wind function relationship modeled by the original, non-seasonal Penman wind function used in the *Brutsaert and Stricker* [1979] AA model, and expressed mathematically in equation (10).

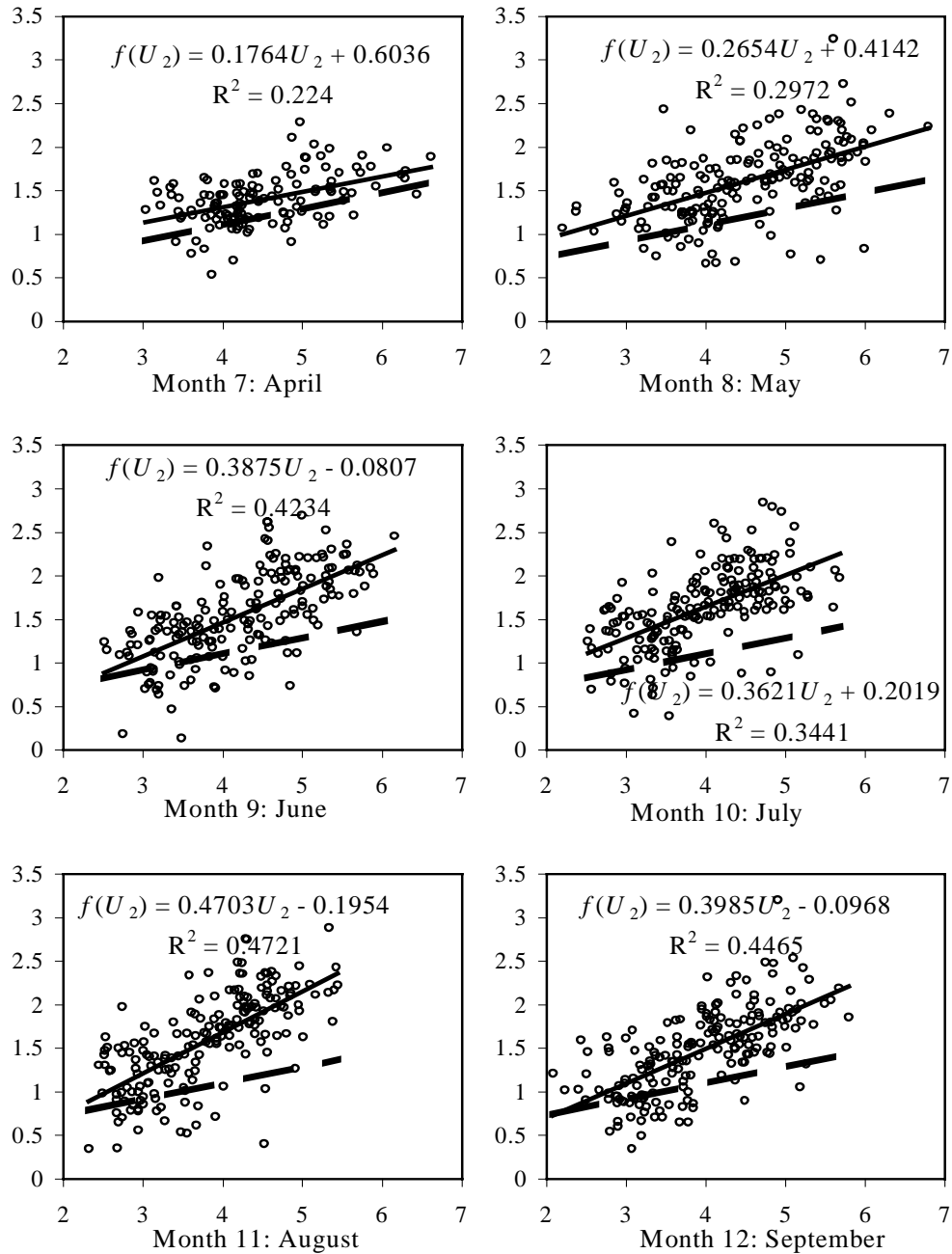


**Figure 4.** (cont.) Monthly  $f(U_2)$ - $U_2$  relationships: months 7-12. Solid line is least-squares fit, with equation and  $R^2$  value indicated. Penman wind function from equation (10) shown by dashed line.

The most significant finding of these relationships (Figure 4) is that the observed  $U_2$ - $f(U_2)$  relationships for the growing season (May through September) are stronger than those predicted by the Penman wind function (10). For a given wind speed, this would have the effect of increasing predicted  $ET_p$ , through an increase in the drying power of the air  $E_a$ . This, in turn, would lead to decreasing estimates of  $ET_a$ . For the rest of the year, the

strength of the observed  $U_2$ - $f(U_2)$  relationship is approximately equal to that of (10), although often slightly offset.

The  $R^2$  values resulting from these relationships do not appear to represent a good fit to the data. The variance of the data points around the line may be explained, at least in part, by two causes. Firstly, the separation between the station recording the climatological data and the observed  $ET_{pan}$ . In many cases, these stations are identical, but for others, the climatological data and  $ET_{pan}$  observations may be separated by up to 1 minute lat/long. Secondly, the  $ET_{pan}$  observations reproduce the  $ET_p$  predicted by the complementary relationship only if the climatological data truly represent the aerological conditions over homogenous upwind areas of scale lengths on the order of 1-10 km. Both of these potential sources of error should induce a normally distributed scatter of points around the best-fit line.

Of primary interest in this study is the performance of the new, seasonally parameterized wind function in the long-term, large-scale water balances outlined earlier. To this end, the AA model is re-coded to reflect the seasonal  $f(U_2)$  expressions (henceforth the modified model is referred to as the AA\* model, and the unmodified model as the AA model), and the water balance closure errors ( $\epsilon^{AA*}$ ) are re-calculated. Figure 5 shows a histogram of the water balance closure errors for the AA\* model. Included for comparison is the histogram for the unmodified AA model.

Given that annual evapotranspiration totals in the annual cycle are highly skewed towards warmer months, the effects of the difference between the annual Penman wind function in equation (10) and the seasonal wind functions upon the long-term, large-scale water balances should be

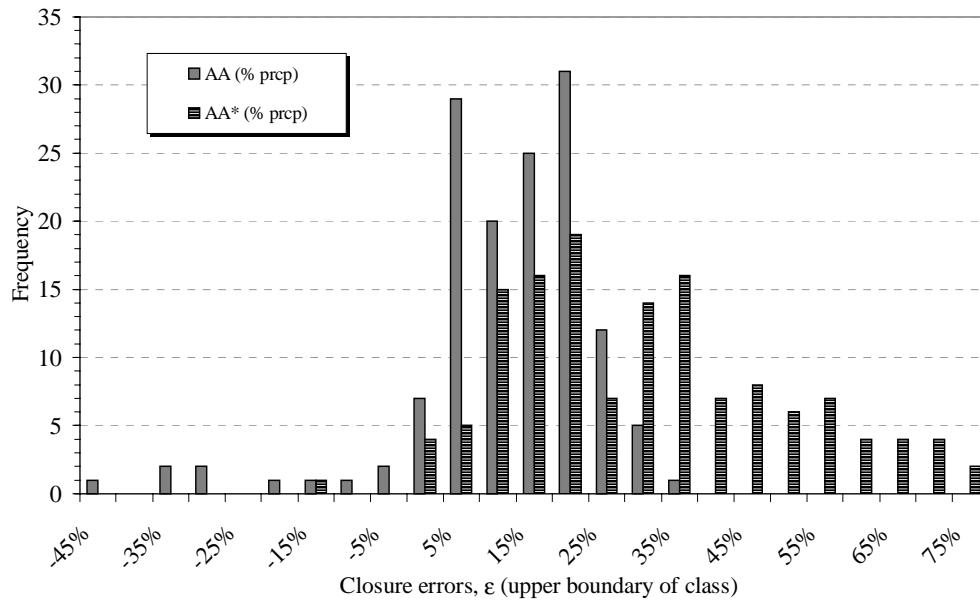


**Figure 5.** Distribution of water balance closure errors,  $\epsilon^{AA}$  and  $\epsilon^{AA*}$ .

significant. One should expect to find that the increases in  $ET_a$  during the months December to February are insignificant when compared to the reductions in  $ET_a$  during the rest of the year. This should lead to increasingly positive water balance closure errors across the study basins.

Figure 5 indicates that this is indeed the case. The histogram of closure errors for the AA\* model has shifted significantly to the right, indicating that it is under-predicting  $ET_a$  as compared to the AA model. The mean closure error has increased from 12.89% to 27.56%. The maxima and minima also indicate this shift: from 30.11% to 74.21% and  $-48.71\%$  to  $-16.47\%$ , respectively. The standard deviation of the AA\* model also compares poorly: 18.91% vs. 12.71% for the AA model.

Finally, in Figure 6, the water balance closure errors for the AA\* model are shown plotted against mean annual wind speed. Included for comparison is the relationship already established for the AA model. The most striking feature of this plot is that the closure errors for the AA\* model bear a significantly stronger relationship to wind speed than for the AA model. Below about 3.8 m/sec, the  $\epsilon^{AA*}$  appear to be independent of wind speed. However, above 3.8 m/sec, the  $\epsilon^{AA*}$  are strongly correlated with wind speed. Thus, for a given wind speed, the AA\* model is over-predicting  $ET_p$  and hence under-predicting  $ET_a$  to a greater degree than the AA model. This plot reinforces the notion that the wind function requires re-parameterization. It is important to remember that only the formulation of  $ET_p$  has been affected by this re-parameterization: as *Katul and Parlange [1992]* suggest, it may be desirable to modify the formulation of the  $ET_w$  component of the complementary relationship.

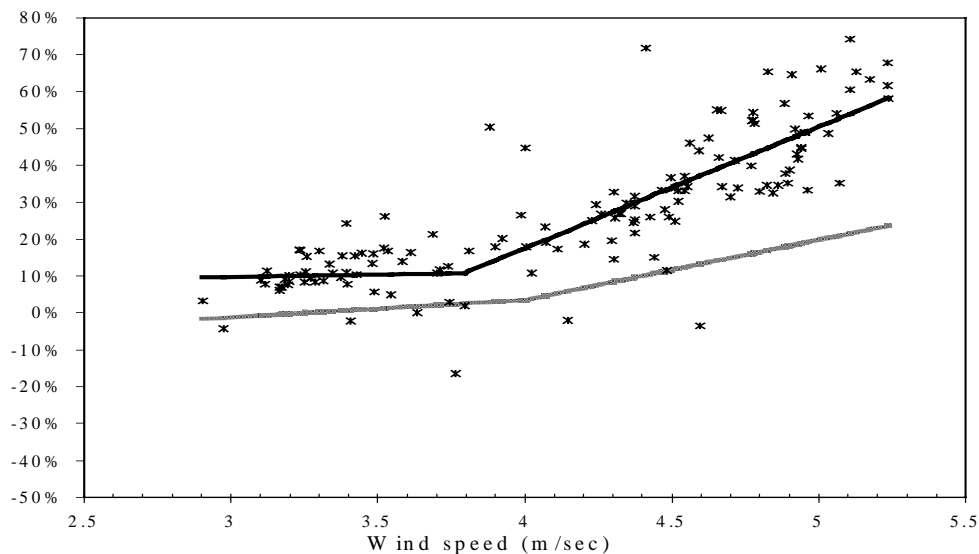


**Figure 6.** Relationships of  $\epsilon^{AA*}$  (x) to mean annual basin-wide wind speed. Regression lines (black for  $\epsilon^{AA*}$ , and grey for  $\epsilon^{AA}$ ) are for trend observations only.

## CONCLUSIONS

The complementary relationship in regional evapotranspiration can be a powerful tool for providing independent estimates of  $ET_a$ . Over homogenous areas at regional scales, these complementary relationship models are preferred over traditional evapotranspiration models using land-based parameterizations, as their data requirements are significantly lighter, and they require no local calibration of parameters.

The CRAE model provides estimates of  $ET_a$  that yield unbiased water balance closure errors, with a variance significantly less than that of the AA model. However, both models' performances are affected by basin climatology (see Figure 7). The CRAE model underestimates  $ET_a$  slightly in humid climates, and overestimates slightly in arid climates, whereas the AA model underestimates  $ET_a$  in all but the most arid climates.

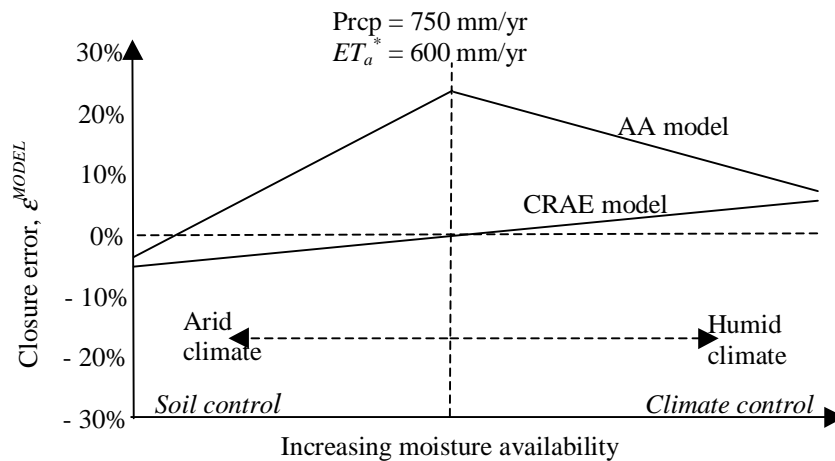


**Figure 7.** Conceptualization of model performance.

Before the AA model can be successfully applied in regional water balances,  $f(U_2)$  must be re-parameterized for accurate  $ET_p$  estimates, and unbiased water balance estimates on a monthly basis. An  $f(U_2)$ -improved AA model is preferred over the CRAE model, as the former uses observed advection data in  $f(U_2)$ , while the latter relies on a constant vapor transfer function  $f_T$ .

Although the use of  $ET_{pan}$  data to derive seasonal wind functions represents an independent means of re-parameterizing the formulation of the  $ET_p$  component of the complementary relationship, as presented it does not produce any improvement in the treatment of advection in the model. In fact, the modified model performs significantly worse than with the original Penman wind function. This is most likely due to experimental procedure. The stations recording the  $ET_{pan}$  may have been too far removed from the stations recording the aerological conditions. Many stations over much of the study area do not record  $ET_{pan}$  data outside of the growing season, leading to a paucity of data points and a spatial bias in the  $ET_{pan}$  data used for these periods. The assumption that the data from the SAMSON stations accurately represent aerological conditions over homogenous areas large enough for the complementary relationship to hold is weak and easily violated.

An alternative approach to re-parameterize the wind function is to minimize the water balance closure error  $\epsilon^{AA}$ . This entails optimizing the wind function on a monthly basis to yield normally distributed closure errors  $\epsilon^{AA}$  with zero mean and minimum variance. This option should minimize errors resulting from study methodology (e.g., poor spatial interpolation techniques, poor data quality). This is not the preferred option, being the least physically based.

## REFERENCES

- (1) Allen, R.G. A Penman for all seasons. *J. Irrig. and Drain. Eng.*, 112(4): 348-368, 1986.
- (2) Bouchet, R.J. Evapotranspiration réelle évapotranspiration potentielle, signification climatique. Int Assoc. Sci. Hydrol., Proceedings, Berkeley, Calif., Symp. Publ. 62: 134-142, 1963.
- (3) Brutsaert, W., and H. Stricker. An advection-aridity approach to estimate actual regional evapotranspiration. *Water Resour. Res.*, 15(2): 443-450, 1979.
- (4) Daly, C., R.P. Neilson, and D.L. Phillips. A statistical-topographic model for mapping climatological precipitation over mountainous terrain, *Journal of Applied Meteorology*, 33(2): 140-158, 1994.
- (5) EarthInfo. NCDC Summary of the Day [TD-3200 computer file]. Boulder, Colorado, U.S.A., 1998a.
- (6) EarthInfo. NCDC Surface Airways [TD-3280 computer file]. Boulder, Colorado, U.S.A., 1998b.
- (7) Gutman, G. A simple method for estimating monthly mean albedo from AVHRR data. *Journal of Applied Meteorology*, 27(9): 973-988, 1988.
- (8) Katul, G.G. and M.B. Parlange. A Penman-Brutsaert Model for wet surface evaporation, *Water Resour. Res.*, 28(1):121-126, 1992.
- (9) Morton, F.I. Operational estimates of areal evapotranspiration and their significance to the science and practice of hydrology, *J. Hydrol.*, 66: 1-76, 1983.
- (10) NREL. Solar and Meteorological Surface Observation Network, 1961-1990. National Renewable Energy Laboratory, Golden, Colorado, U.S.A., 1993.
- (11) Parlange, M.B., and G.G. Katul. Estimation of the diurnal variation of potential evaporation from a wet bare soil surface. *J. Hydrol.*, 132: 71-89, 1992a.
- (12) Parlange, M.B., and G.G. Katul. An advection-aridity evaporation model. *Water Resour. Res.*, 28(1): 127-132, 1992b.
- (13) Penman, H.L. Natural evaporation from open water, bare soil and grass, *Proc. R. Soc. London, Ser. A.*, 193: 120-146, 1948.
- (14) Priestley, C.H.B., and R.J. Taylor. On the assessment of surface heat flux and evaporation using large-scale parameters, *Monthly Weather Review*, 100: 81-92, 1972.
- (15) Ramírez, J.A., and L. Claessens. Large scale water budgets for the United States, Hydrologic Science and Engineering Department, Colorado State University, Final Progress Report Cooperative Agreement No. 28-C2-618, Fort Collins, Colorado, U.S.A., 153 pp., 1994.
- (16) Slack, J.R., and J.M. Landwehr. Hydro-Climatic Data Network (HCDN): Streamflow Data Set, 1874-1988. U.S. Geologic Survey, open-file report 92-129, 1992.
- (17) Van Bavel, C.H.M. Potential evaporation: the combination concept and its experimental verification, *Water Resour. Res.*, 2(3): 455-467.
- (18) Wright, J.L. New evapotranspiration crop coefficients. *J. Irrig. and Drain. Div.*, ASCE, 108(IR2): 57-74, 1982.